

## Effect of Stable Layer Formation over the Po Valley on the Development of Convection during MAP IOP-8

HEATHER DAWN REEVES AND YUH-LANG LIN

*Department of Marine, Earth, and Atmospheric Sciences, North Carolina State University, Raleigh, North Carolina*

(Manuscript received 31 January 2005, in final form 22 December 2005)

### ABSTRACT

During intensive observation period (IOP)-8 of the Mesoscale Alpine Program, there was a stable layer of air in the lowest levels of the Po Valley and just upstream of the Apennines. In this study, the effects of the stable layer on the formation of convection in the southern Alpine region were investigated through a series of two-dimensional, idealized experiments. The goals of this study were twofold: 1) to determine if stable layer strength affected the placement of convection and 2) to test the notion that the stable layer during IOP-8 behaved as an effective mountain. To accomplish the first objective, three simulations were compared in which the strength of the inversion and low-level cooling in the Po Valley and upstream of the Apennines was varied. The results of these simulations show that the stronger the inversion and low-level cooling, the farther south the convection was positioned. Additionally, it was found that convection developed as a result of the formation of a broad region of moist instability over the stable layer. Cellular convection developed in this region of moist instability. The second objective was tested through a simulation where the cold pool was replaced by terrain (MMTN). As in the reference (or STB10) simulation, the upslope of the terrain in the MMTN simulation was characterized by a wide zone of moist instability. However, wave structures to the lee of the Apennines were markedly different in the STB10 and MMTN simulations. This led to different convective and precipitation patterns, with the MMTN simulation exhibiting heavier convection over the Po Valley while the heaviest convection in STB10 was upstream of the Apennines. These results suggest that, at best, the stable layer in the STB10 simulation can only be roughly approximated by terrain.

### 1. Introduction

In the fall of 1999, a field program, called the Mesoscale Alpine Program (MAP; Bougeault et al. 2001), took place in the southern Alpine region of the Po Valley (Fig. 1). One main objective of MAP was to identify and better understand the mechanisms that generate or enhance heavy orographic precipitation. One of the intensive observation periods (IOPs) of MAP, IOP-8, has been the subject of numerous journal articles (Bousquet and Smull 2003; Medina and Houze 2003; Rotunno and Ferretti 2003; Steiner et al. 2003; Lin et al. 2005) and conference preprints because the predominantly stratiform nature of the precipitation during IOP-8 flies contrary to the forecasts, which called for deep, heavy convection over the Po Valley

and southern slopes of the Alps (Bousquet and Smull 2003; Rotunno and Ferretti 2003).

Through analysis of the soundings at Milan during IOP-8, Medina and Houze (2003) have concluded that the air in the Po Valley lacked sufficient kinetic energy to ascend the barrier presented by the Alpine massif. Hence, there was no deep, penetrative convection over the Po Valley or southern slopes of the Alps during IOP-8. Bousquet and Smull (2003) noted that convection did occur during IOP-8, but it was located over the northern Ligurian Sea, about 200 km south of where it was forecast to occur. Through inspection of soundings from the P3 drop-sounding and Ajaccio, they determined there was a convergence zone located over the northern Ligurian Sea. They argued this convergence may have acted to trigger the convection over the Ligurian Sea. Furthermore, it was suggested in Bousquet and Smull (2003) that the convection over the Ligurian Sea depleted moisture from the atmosphere, thus leading to decreased moisture availability and decreased convection over the Po Valley and southern slopes of

---

*Corresponding author address:* Heather Dawn Reeves, Dept. MEAS, 1125 Jordan Hall, Faucette Drive, NCSU, Raleigh, NC 27695-8208.  
E-mail: hdreeves@unity.ncsu.edu

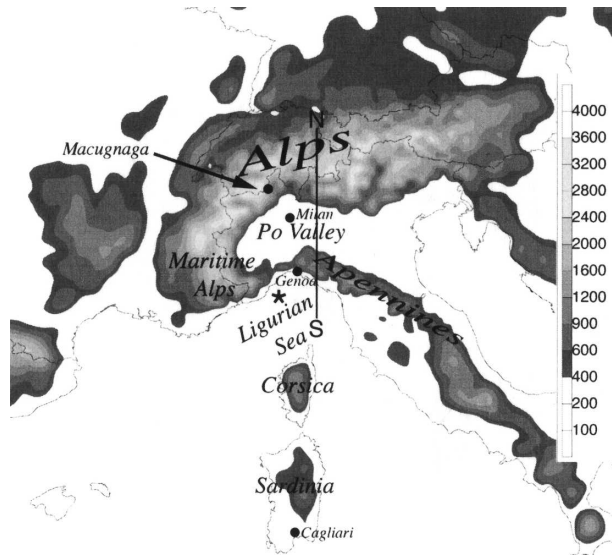


FIG. 1. Alps topography (shaded as in legend) showing Cagliari, Genoa, Milan, and Macugnaga. The star denotes the location of the P3 dropsonde. Line NS represents the cross section shown in Fig. 2.

the Alps. This conclusion was further supported in the analyses and numerical simulations of Lin et al. (2005).

Observations of IOP-8 indicate there was a cool, moist layer of air capped by a strong inversion extending across the lowest 2 km of the Po Valley and southward over the northern Ligurian Sea during IOP-8 (Bousquet and Smull 2003; Medina and Houze 2003; Rotunno and Ferretti 2003). As will be demonstrated in section 2, the Mesoscale Compressible Community Model (MC2) forecasts underestimated the strength of the inversion at the top of the cold pool. Smull et al. (2001) explored, with inconclusive results, whether or not the misforecast in stable layer strength was related to the misforecast of the placement of convection. Herein, we further explore that hypothesis.

Lin et al. (2005) contended that the stable layer behaved as a material surface such that airstreams impinging upon the stable layer from the south rose over it as though rising over terrain. For this reason, they argued that the stable layer behaved as an effective mountain (Rottman and Smith 1989; Rotunno and Ferretti 2001). The trajectory analyses presented in Rotunno and Ferretti (2003, see their Fig. 8f) also support this notion, showing the southerly airstream as having been abruptly lifted as it encountered the leading edge of the cold dome. Lifting by the effective mountain was hypothesized by Lin et al. (2005) to be the main trigger for convection over the Ligurian Sea. Although their numerical simulations and analyses support the idea that

the stable layer behaved as an effective mountain, a more rigorous test of this hypothesis has yet to be presented.

The objectives of this paper are to 1) see if the placement of convection is altered for different stable layer strengths and 2) further test the effective mountain hypothesis. To accomplish the goals of this paper, we have performed a series of two-dimensional, idealized experiments utilizing an upstream sounding from the stable layer during IOP-8 for the initial conditions. Using this approach, we are able to isolate the effects of the stable layer on the formation of convection from other forcings that were present in the real atmosphere. This paper is organized as follows. In section 2, we present a brief overview of the observations and forecasts from IOP-8. In section 3, we follow with a description of the experimental design. The effect of inversion strength on the formation and placement of convection is discussed in section 4. In section 5, the effective mountain hypothesis is tested. Finally, conclusions are discussed in section 6.

## 2. Case overview

We first start with a cursory overview of the sequence of events as they occurred during IOP-8. This particular IOP was associated with a large-scale baroclinic zone and upper-level trough that approached the southern Alpine region from the west (Lin et al. 2005; see their Figs. 2 and 3). Several hours before the southerly winds associated with the eastward moving trough impinged on the south face of the Alpine ridge, easterly winds at low levels advected air with relatively high static stability and moisture content into the Po Valley (Rotunno and Ferretti 2003). This advection, which continued throughout the remainder of the IOP, resulted in the development of a relatively stable layer of air in about the lowest 2 km of the Po Valley (Medina and Houze 2003). Inspection of Fig. 2a, which shows a vertical cross section along  $9.5^{\circ}\text{E}$  of equivalent potential temperature ( $\theta_e$ ) and relative humidity from the MC2 forecast model initialized at 2100 UTC 20 October 1999 (panel marked 10/20/21Z), reveals that the MC2 forecast did anticipate a stable layer in the Po Valley at 0000 UTC 21 October. Model forecast stable conditions existed only within the Po Valley and just a few kilometers upstream of the Apennines. Later output times (Figs. 2b–d) from this same forecast run show a convective system was forecast to develop over the peak of the Apennines and propagate northward over the Po Valley. The MC2 forecast initialized at 2100 UTC 19 October was similar to that at 2100 UTC 20 October with the exception that the stable layer in this earlier forecast was weaker while

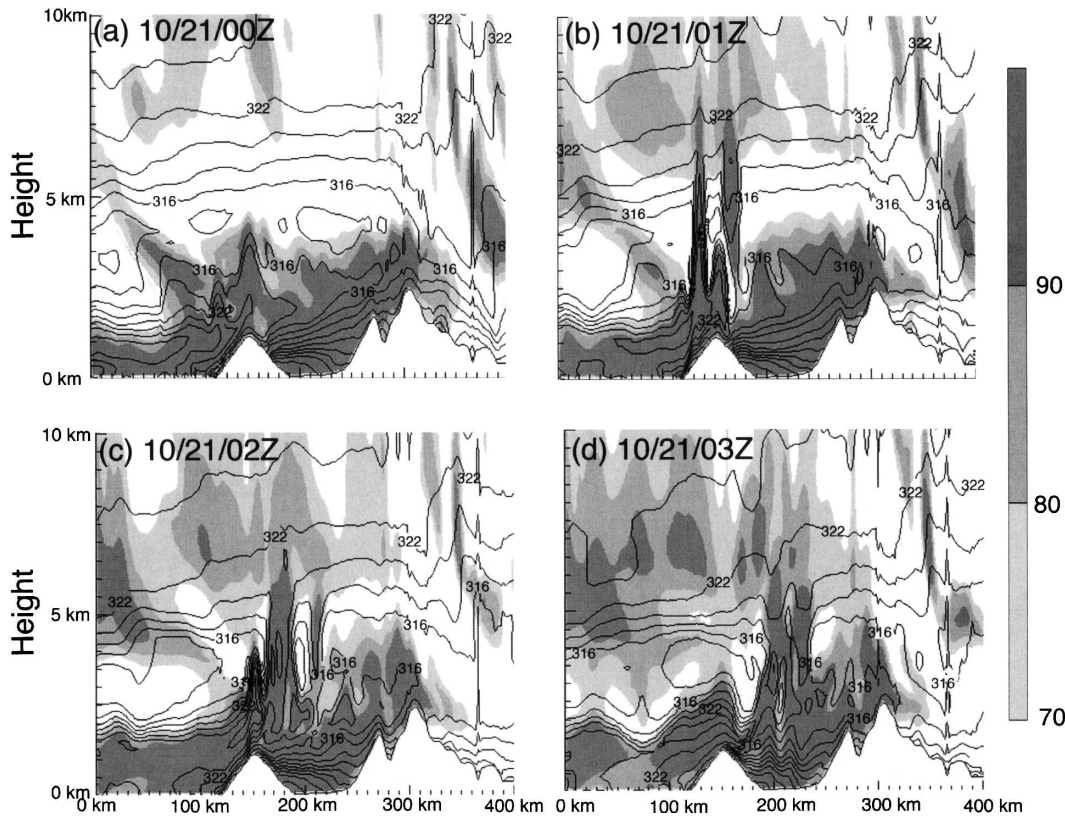


FIG. 2. Cross section along  $9.5^{\circ}\text{E}$  longitude (see Fig. 1) from the MC2 model forecast initialized on 2100 UTC 20 Oct 1999 showing equivalent potential temperature (contoured) and relative humidity (shaded as in legend).

the convective system was stronger. Both the Swiss model and the MC2 model anticipated significant precipitation accumulations on the upslopes of the Alps (120 mm for the 24 h ending at 0000 UTC 22 October) in association with this convective system (Bousquet and Smull 2003).

The sequence of events did not materialize as the forecast models anticipated. Figure 3a, which shows a rain gauge analysis from 1200 UTC 20 October to 2200 UTC 21 October, indicates the accumulations were significantly less than those forecast with rather modest accumulations in the Po Valley and on the mountain upslopes. The radar reflectivity cross section, obtained from a composite of radars used during the special observation period [SOP; see Bousquet and Smull (2003) for more details] shown in Fig. 3b, also shows the nature of the precipitation over the Po Valley was more-or-less stratiform and, additionally, shows there was deep convection just off the Ligurian coast. The same convective structure can be discerned from satellite imagery (see Fig. 4 of Lin et al. 2005).

Although the precipitation over the Po Valley and upslopes of the Alps has been found to be predominantly stratiform, there is evidence that shallow convec-

tion existed over the upslopes of the Alps. Figure 3c shows a time series of vertical velocities obtained from the vertically pointing antenna on the Swiss Federal Institute of Technology (ETH) X-band vertically pointing (VP) radar, deployed from Macugnaga (Fig. 1). Below about 2 km, the cloud was essentially stratiform with a well-defined bright band at 2 km (see Fig. 21a of Houze and Medina 2005). Conversely, the layer between 4 and 6 km shows there were pulses in the wind field with a period of about 4.5 min. These pulses are similar to those observed in cases of cellular convection associated with moist instability (Crook and Moncrieff 1988; Kirshbaum and Durran 2004; Furber and Schär 2005). Houze and Medina (2005) argue this convective pattern is the result of shear instability.

Figures 4a–c show the observed soundings at 0000 UTC 21 October from Milan and Genoa and from the P3 drop-sounding at 0800 UTC 21 October. The Milan sounding (Fig. 4a) shows a very strong inversion was present over the Po Valley at about 800 hPa. Inversions were also present in the Genoa and P3 soundings (Figs. 4b,c) at about 900 hPa. Soundings from the MC2 forecast starting at 2100 UTC 20 October have been plotted in Figs. 4d–f. These soundings show that although an

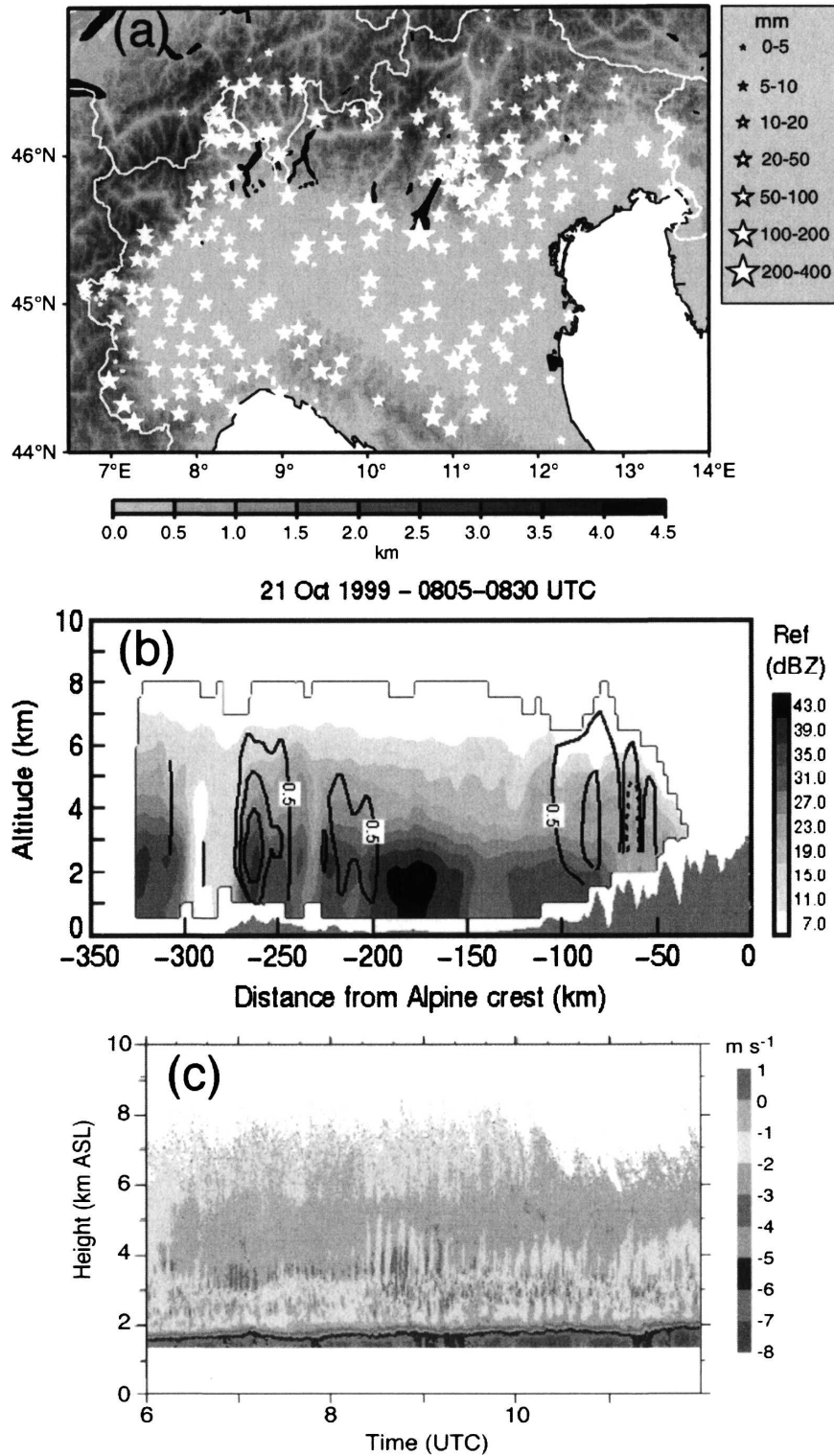


FIG. 3. (a) Accumulated precipitation from 1200 UTC 20 October to 2200 UTC 21 October (adapted from Medina and Houze 2003), (b) meridional cross section showing radar reflectivity (see legend to right of panel) and positive vertical velocity in steps of  $0.5 \text{ m s}^{-1}$  starting at  $0.5 \text{ m s}^{-1}$  (adapted from Bousquet and Smull 2003), and (c) radar derived vertical velocity obtained from the ETH X-band VP radar deployed from Macugnaga from 0600 to 1200 UTC 21 October (adapted from Houze and Medina 2005).

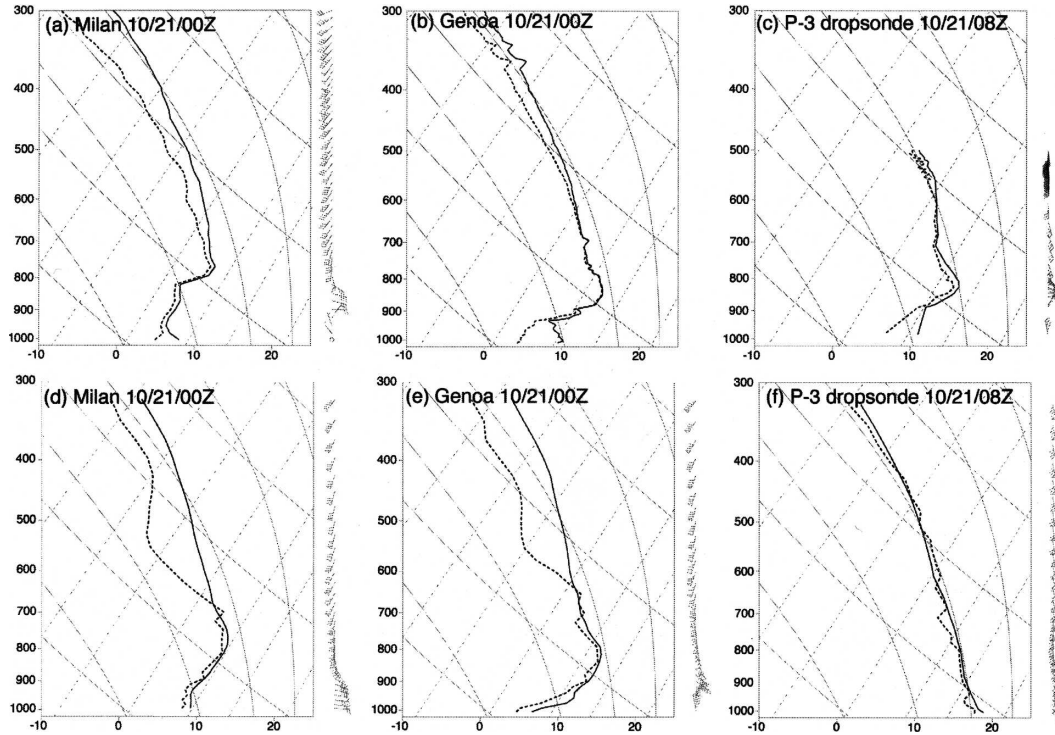


FIG. 4. Observed skew  $T$ -log  $p$  soundings from (a) Milan, (b) Genoa, and (c) the P-3 dropsonde, and MC2 model forecast soundings for (d) Milan, (e) Genoa, and (f) the P-3 dropsonde location.

inversion was forecast at Milan and Genoa by the MC2 model, its strength was significantly weaker than in the observations. No inversion was forecast at the P-3 dropsonde location (Fig. 4f). The comparison of the observed soundings with the MC2 forecast soundings indicates that both the strength and horizontal extent of the stable layer were not adequately forecast.

### 3. Experimental design

Simulations were performed using the Advanced Regional Prediction System (ARPS) used for the International H<sub>2</sub>O Project (ARPS-IHOP5; Xue et al. 2001). This model solves the fully compressible, three-dimensional, nonhydrostatic equations. Terrain-following height coordinates were used in these simulations. Fourth- and second-order advection schemes were used in the horizontal and vertical directions, respectively. The horizontal grid spacing is 2 km and the horizontal domain has 512 grid points in the north-south direction and 4 grid points in the east-west direction. The vertical grid spacing is stretched from 40 m in the lowest 2000 m of the domain to 370 m at the domain top. There are 120 vertical levels, which gives a domain height of 18 km. A sponge layer was applied above 14 km to reduce artificial wave reflection by the

upper boundary. The boundary conditions in the east and west directions were periodic. These periodic conditions, along with the fact that the domain was very narrow in the  $y$  direction, allow for the simulation to be effectively two-dimensional. A radiation boundary condition was used for the north and south boundaries. The lower boundary was free slip. Microphysical processes were handled using a parameterization scheme based on Lin et al. (1983). In all simulations, the model time step is 3 s and each simulation was integrated for 25 h. The Cagliari sounding, which was upstream of the effective mountain, at 0000 UTC 21 October (IOP-8; Fig. 5) was used with a uniform southerly wind of 10 m s<sup>-1</sup> to initialize all simulations.

The Alps and Apennines are represented by two-dimensional mountain geometry given by

$$h(y) = h_m \exp \left[ - \left( \frac{y - y_0}{a} \right)^2 \right], \quad (1)$$

where  $h(y)$  is the terrain height function,  $h_m$  is the maximum terrain height (2000 m for the Alps and 1000 m for the Apennines), and  $a$  is the half-width (30 km for the Alps and 10 km for the Apennines). The distance between the peaks of the Alps and Apennines is 200 km (see Fig. 6). The mountains were introduced impulsively into the domain at  $t = 0$  s.

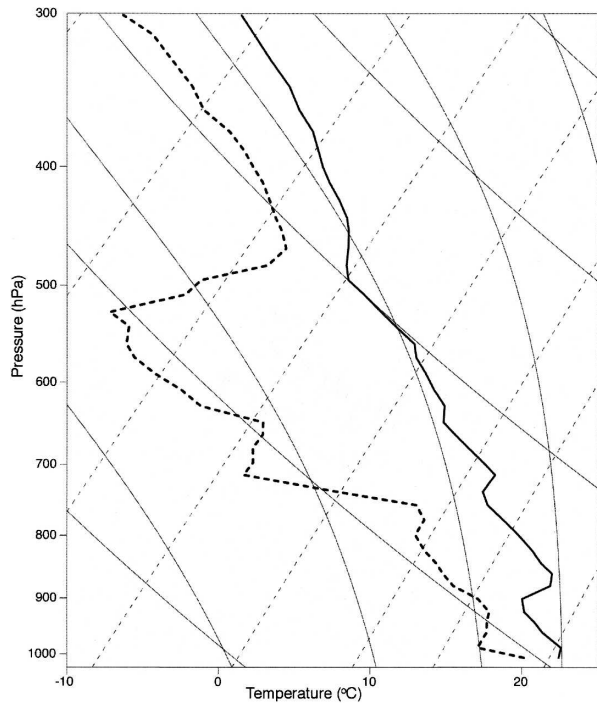


FIG. 5. Input sounding on a skew  $T$ -log  $p$  diagram for idealized simulations. Sounding is from Cagliari at 0000 UTC 21 October.

#### 4. Effect of inversion and stable layer strength

##### a. Comparison of simulations with differing stable layer strength

We first start with a comparison of three simulations with varying inversion and cold pool strengths. These are the STB10, STB5, and 2MTN simulations. In STB10 (STB5) there was an initial cool layer of  $-10$  K ( $-5$  K) in the Po Valley and upstream of the Apennines (shown as the shaded area in Fig. 6). The cooled region approximates the shape of the cold dome in the observations and previous numerical simulations of IOP-8 (Lin et al. 2005). It should be noted that in order to avoid a supersaturated layer of moist instability, the specific humidity was decreased in this region by  $4.5$  g  $\text{kg}^{-1}$  for the STB10 simulation and  $1.5$  g  $\text{kg}^{-1}$  for the STB5 simulation. A certain adjustment time is expected given these initial conditions. However, such an adjustment is not entirely unrealistic as the stable layer in the actual event was present several hours before the southerly winds impinged on it (Lin et al. 2005). Additional cooling at a rate of  $50$  K  $\text{day}^{-1}$  was imposed in the shaded region to represent the continued feed of cool, moist air into the Po Valley that was observed during IOP-8 (Rotunno and Ferretti 2003; Steiner et al. 2003). This value is consistent with the observed cooling rates for IOP-8 listed in Steiner et al. (2003) and

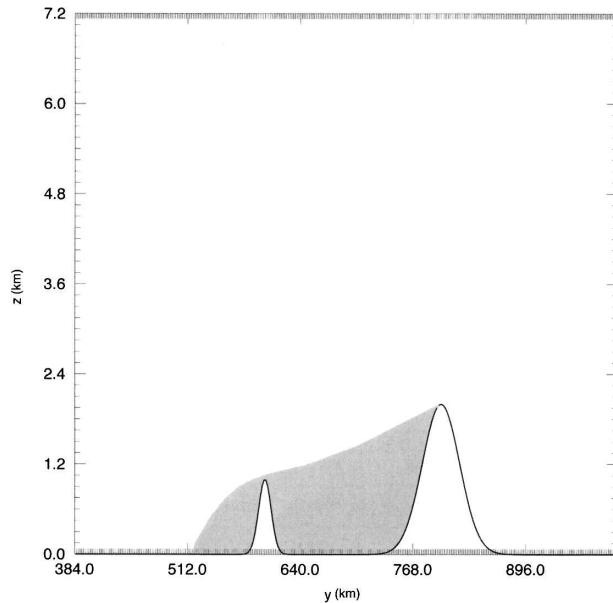


FIG. 6. Idealized mountain geometry for idealized simulations. The shaded area represents regions of cooling for some simulations as discussed in text.

Bousquet and Smull (2003) of  $1.8$  K  $\text{h}^{-1}$ . Given that there is continued cooling in the STB10 and STB5 simulations, a steady-state solution is not expected (Smith and Lin 1982). In the 2MTN experiment, no cooling, either initially or at later times during the simulation, was imposed in the Po Valley or upstream of the Apennines.

Figure 7a shows a Hovmöller diagram of rain rate for the 2MTN simulation. Convection was apparent over the Alps (located at  $y = 800$  km) as is indicated by the narrow bands of enhanced rain rate. Although the whole system is quasi-stationary over the peak of the Alps, individual cells propagated upstream during the time period between 13 and 21 h. After 21 h, individual cells propagated downstream. Over the Apennines (located at  $y = 600$  km), there is no evidence of convective activities. The accumulated precipitation (Fig. 7b) echoes the convective pattern revealed in Fig. 7a, with a precipitation maximum of  $135$  mm over the peak of the Alps and only trace amounts of precipitation in the Po Valley.

A more complete picture of the convective activities in the 2MTN simulation is provided in Fig. 8, which shows  $\theta$ ,  $w$ , and total water mixing ratio ( $q_{\text{tot}}$ ) at  $t = 20$  h. There was weak lifting on the upstream side of the Apennines that resulted in the formation of a cap cloud over the mountain peak. To the lee of the Apennines, there was a strong downslope wind and a stationary hydraulic jumplike feature. This “jump” did not significantly alter the thermodynamic conditions downstream

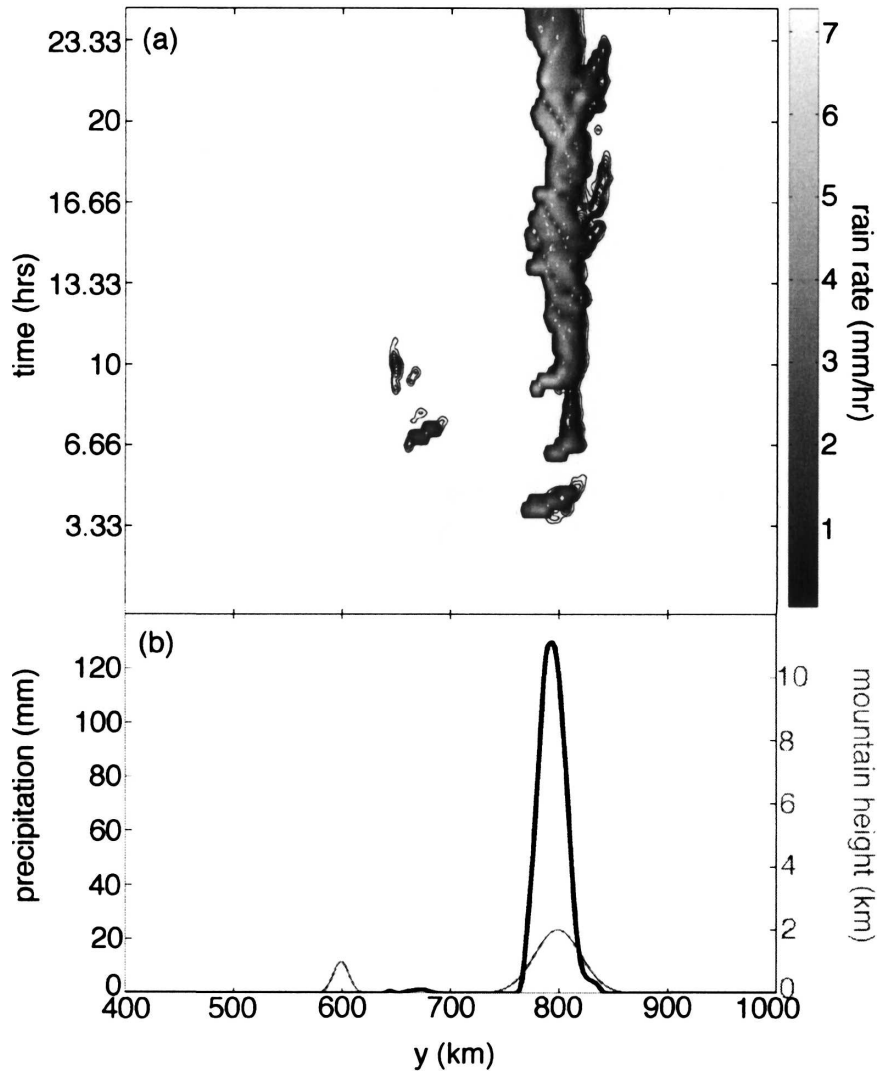


FIG. 7. (a) Hovmöller diagram of rain rate (shaded as in legend) and (b) 25-h accumulated precipitation (black curve) and orography (gray curve) for the 2MTN simulation.

of 700 km. A comparison of the input sounding (Fig. 5) to that at 700 km and  $t = 20$  h (not shown) shows the soundings are nearly identical. Over the Alps, there was a stratiform cloud with embedded convection.

Figure 9a shows a Hovmöller diagram of rain rate for the STB5 simulation. Comparison of this figure with Fig. 7a, which shows the Hovmöller diagram from the 2MTN simulation, shows that the introduction of the cold pool led to markedly different convective patterns. In STB5 (Fig. 9a), the most vigorous convection was over the Po Valley (between 600 and 800 km) rather than over the peak of the Alps. Another important feature that can be discerned from Fig. 9a is an apparent regime change that occurred at about 13 h. Before this time, the convective systems, which initially developed over the peak of the Apennines, propagated up-

stream reaching as far upstream of the Apennines as  $y = 550$  km. After 13 h, the convective system remained stationary to the lee of the Apennines with individual cells propagating downstream. Notice there was no convection upstream of the Apennines after 13 h. This regime change will be discussed further in section 4b.

The accumulated precipitation in the STB5 simulation (Fig. 9b) shows the greatest accumulation (60 mm) occurred on the upslope of the Alps. Smaller accumulations between 10 and 30 mm existed in the southern Po Valley. There was very little precipitation upstream of the Apennines.

Figure 10 shows  $\theta$ ,  $w$ , and  $q_{\text{tot}}$  at  $t = 10$  and 20 h for the STB5 simulation. This figure shows that between 10 and 20 h, the stable layer upstream of the Apennines was eroded. This behavior is consistent with the find-

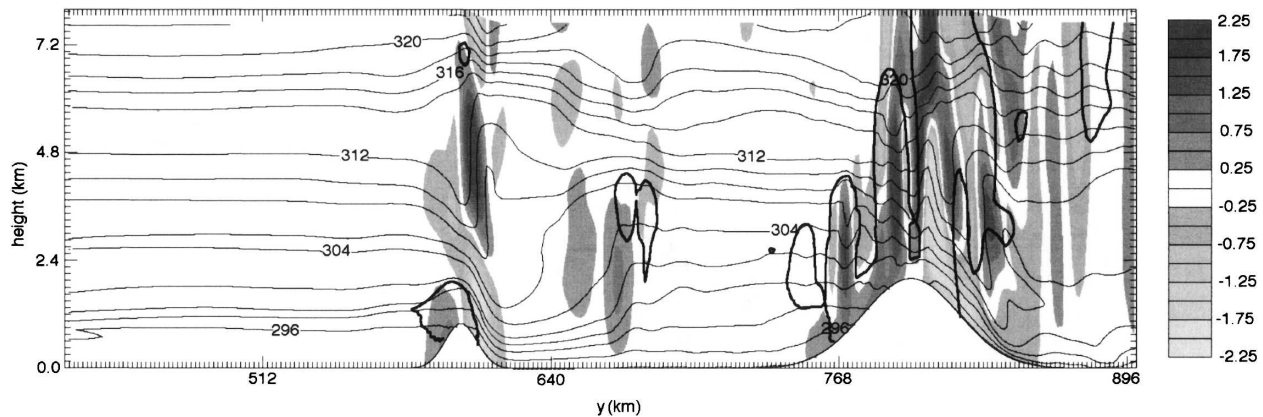


FIG. 8. Vertical cross section of potential temperature (thin contours), vertical velocity (shaded as in legend), and total liquid, ice, and snow mixing ratio =  $0.03 \text{ g kg}^{-1}$  (thick contours) at  $t = 20 \text{ h}$  for the 2MTN simulation.

ings of Raymond and Rotunno (1989) and Xu et al. (1996) who noted that for supercritical flow, the nose, or leading edge, of the density current becomes tapered and flattened with time. The erosion of the cold pool upstream of the Apennines in STB5 is also in agreement with Zängl (2003) who found that stable layers upstream of orography tend to be eroded by advection more quickly than sheltered cold pools.

Even though the cold pool in the Po Valley was sheltered by the Apennines in the STB5 simulation, erosion did occur. This appears to be directly related to the strength of the low-level stable layer. In his studies, Zängl (2003, 2005) found that the nature of cold pool erosion was strongly dependent on cold pool strength. For weak or moderate stability, downward motion to the lee of the sheltering orography acted to advect the stable layer out of the basin. Such a mechanism appears to have been responsible for the eroded stable layer in this simulation.

Figure 11a shows a Hovmöller diagram of rain rate for the STB10 simulation. Weak convective activities are apparent over the Po Valley after 6 h. Vigorous convection was triggered upstream of the Apennines at about 15 h. Although this convective system was stationary, individual cells propagated downstream. The accumulated precipitation for the STB10 simulation (Fig. 11b) has a maximum of 35 mm upstream of the Apennines and maximum of 40 mm on the upslopes of the Alps. This precipitation distribution is consistent with the observations of IOP-8. Although we cannot confirm the maximum present south of the Apennines in the STB10 simulation actually existed during the real event, since this location is over the Ligurian Sea, the synoptic data presented and discussed in section 2 (Figs. 3b,c) as well as analyses presented in Bousquet and Smull (2003) and Lin et al. (2005) do indicate there

was deep convection over the Ligurian Sea during IOP-8. Therefore, it is not unreasonable to assume there was a localized maximum of precipitation upstream of the Apennines in the real case.

A cross section of  $\theta$ ,  $w$ , and  $q_{\text{tot}}$  from the STB10 simulation at 20 h is shown in Fig. 12. At this time, the stable layer, although somewhat modified in shape, is still very much intact both upstream of the Apennines and over the Po Valley. This is consistent with the observations of IOP-8. The lack of erosion to the stable layer to the lee of the Apennines in STB10 is consistent with the findings of Lee et al. (1989) and Zängl (2003, 2005). They showed that wave generation in the presence of a strong leeside cold pool is significantly dampened. They further noted that downward motion to the lee of the mountain is inhibited within the cold layer, thus preventing the cold pool from being advected away from the mountain.

In Fig. 12, cellular convection is apparent above the leading edge of the stable layer between  $y = 500 \text{ km}$  and  $y = 550 \text{ km}$ . To ensure that this convective development was not due to numerical roundoff error, a simulation identical to the STB10 simulation was performed using double precision. The locations of convective development, the nature of convection, and the precipitation distribution in this simulation were nearly identical to those in the STB10 simulation. This convection upstream of the Apennines was rather shallow, not extending above 5 km. Observations and full-physics simulations of IOP-8 (Bousquet and Smull 2003; Lin et al. 2005) show the convection over the Ligurian Sea as having been deep, extending throughout the troposphere. In an effort to replicate the deep convection upstream of the Apennines, a simulation identical to that in the STB10 simulation was performed only with random thermal perturbations forced

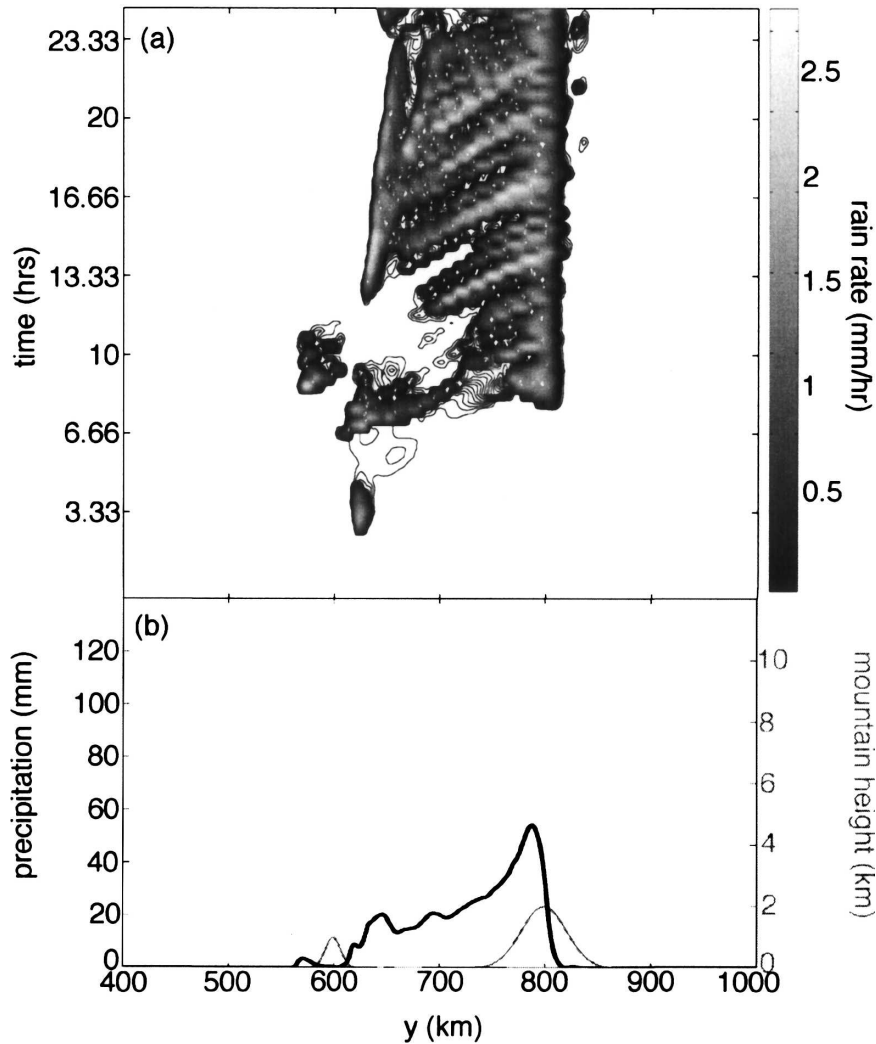


FIG. 9. (a) Hovmöller diagram of rain rate (shaded as in legend) and (b) 25-h accumulated precipitation (black curve) and orography (gray curve) for the STB5 simulation.

into the basic state flow. Deep convection did not develop in this simulation, suggesting that the sounding used herein was too stable to support penetrative convection. The presence of deep convection in the observations of IOP-8 can be explained by the fact that upper-level divergence existed in the real case as well as in the full-physics simulations of Lin et al. (2005). The additional lifting provided by the upper-level divergence may have enhanced the convection over the Ligurian Sea (Lin et al. 2005). Additionally, in the STB10 simulation, we were unable to replicate the northerly winds noted within the stable layer for IOP-8 (Bousquet and Smull 2003; Medina and Houze 2003; Rotunno and Ferretti 2003; Lin et al. 2005) without violating necessary balance constraints for the two-dimensional framework. The convergence of the north-

erly winds within the stable layer with the southerly winds over the Ligurian Sea has been hypothesized to be a major contributor to the convection over the Ligurian Sea (Bousquet and Smull 2003) and may have acted to enhance convection upstream of the Apennines.

Although deep convection was not achieved in the STB10 simulations, thermodynamic profiles downstream of the convection show good agreement with the observations. Figure 13 shows a comparison of the Milan sounding at 0600 UTC 21 October with the STB10 sounding at  $t = 20$  h and  $y = 700$  km. In both the observations and the STB10 simulation, the strength of the inversion was about  $0.03^{\circ}\text{C m}^{-1}$ . Beneath the inversion, the temperature profiles were near neutral and were also saturated. Above the inversion, the tempera-

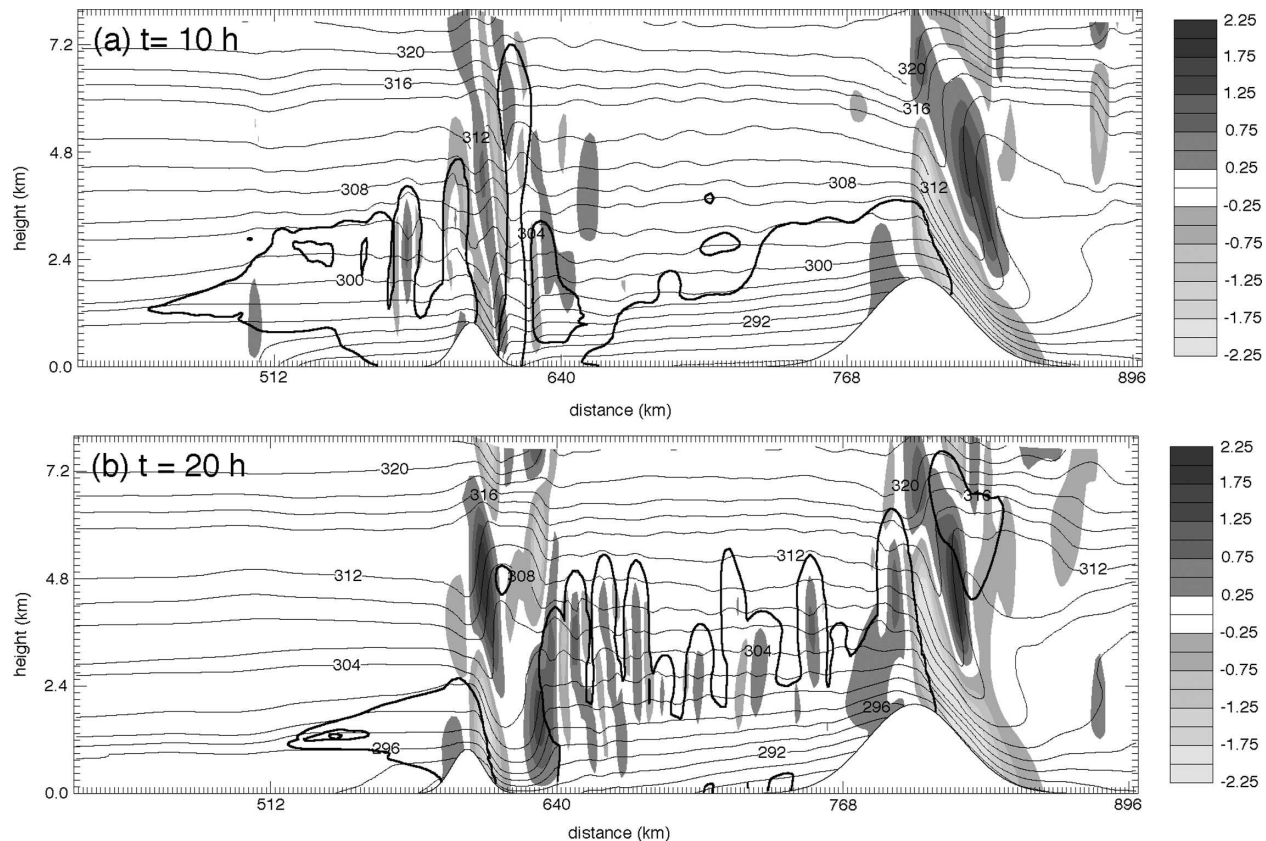


FIG. 10. Vertical cross section of potential temperature (thin contours), vertical velocity (shaded as in legend), and total liquid, ice, and snow mixing ratio =  $0.03 \text{ g kg}^{-1}$  (thick contours) at (a)  $t = 10 \text{ h}$  and (b)  $t = 20 \text{ h}$  for the STB5 simulation.

ture profiles roughly followed the moist adiabatic lapse rate and were near saturation. The observed soundings at Genoa also compare well to soundings taken just upstream of the Apennines from the STB10 simulation (not shown).

To briefly summarize, the 2MTN, STB5, and STB10 simulations indicate that there is a correlation between the strength of the inversion and cold pool in the location of the most intense convection and heaviest precipitation with an increase to stable layer strength associated with a southward shift in convection. Among these three simulations, the STB10 simulation shows the best agreement with the observations: a point that may indicate that the processes important for the formation of convection in the STB10 simulation were also active in the real atmosphere. It is important to note that it is unrealistic to expect cooling rates of  $50 \text{ K day}^{-1}$  to last for 25 h in the real atmosphere. Sensitivity tests with smaller cooling rates had stable layers that did not maintain their shape in the face of the impinging flow. At first blush, this point appears to be a detriment to the application of the results. However, the aim herein was to assess how the development of con-

vection differed for stable layers that remained quasi-stationary versus those that eroded. The conclusion that there appears to be a connection between stable layer strength and the location of convection is still a valid one as far as the two-dimensional simulations are concerned.

#### b. Mechanisms for convection in STB5 and STB10

Figure 14 shows cross sections of equivalent potential temperature ( $\theta_e$ ) and wind vectors at  $t = 9, 11, 13,$  and  $15 \text{ h}$  for the STB10 simulation. Examination of the wind field in Fig. 14 shows that air in the lowest 2 km experienced layerlike lifting as it encountered the leading edge of the stable dome. Crook and Moncrieff (1988) argued that layer lifting can lead to the formation of a region of moist instability wherein the flow is unstable with respect to infinitely small perturbations. Furthermore, they demonstrate that the ensuing convection in such a circumstance takes on the appearance of Rayleigh-Bénard-type convection. Whether or not the convection is due to the formation of a layer of moist instability can be deduced through inspection of the saturated Brunt-Väisälä frequency ( $N_m^2$ ) (Durran and

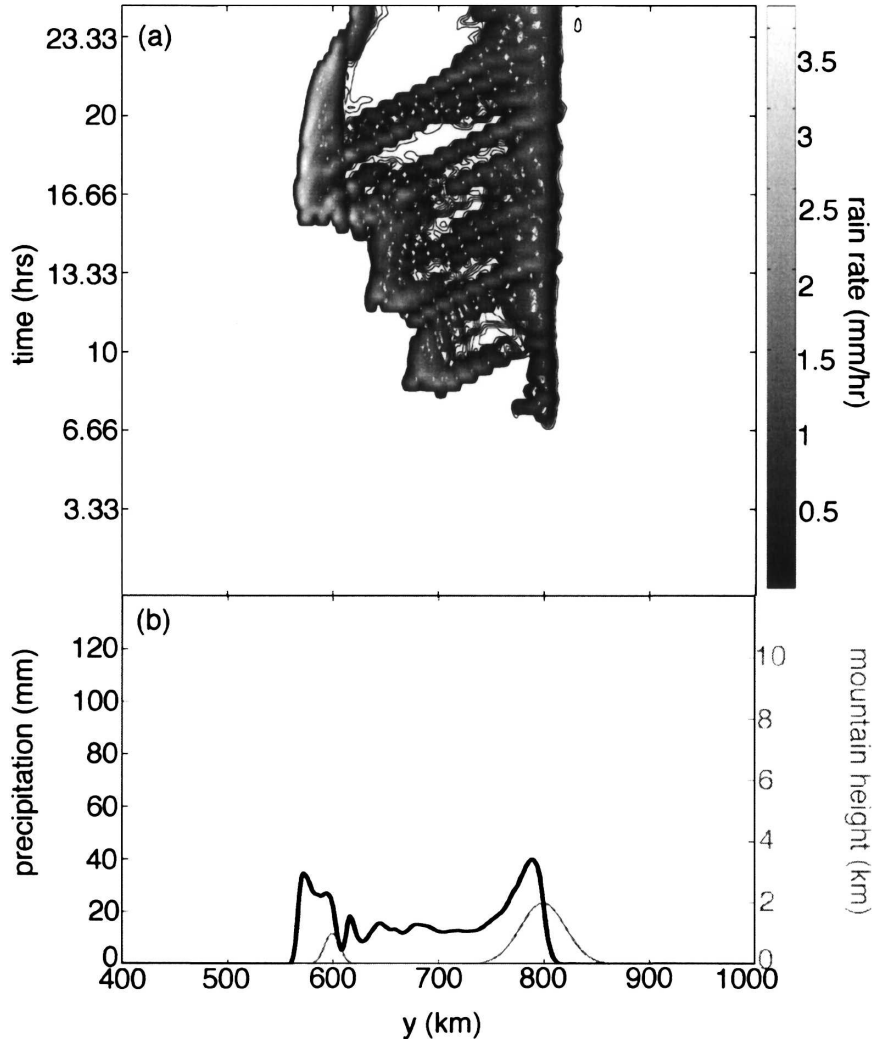


FIG. 11. (a) Hovmöller diagram of rain rate (shaded as in legend) and (b) 25-h accumulated precipitation (black curve) and orography (gray curve) for the STB10 simulation.

Klemp 1982). The formulation for  $N_m^2$  may be written as follows:

$$N_m^2 = \frac{1}{1 + q_w} \left[ \underbrace{\Gamma_m(c_p + c_l q_w) \frac{1}{\theta_e} \frac{\partial \theta_e}{\partial z}}_A + \underbrace{\left( \Gamma_m c_l \ln \frac{\theta_e}{T} - g \right) \frac{\partial q_w}{\partial z}}_B \right], \quad (2)$$

where  $\Gamma_m$  is the moist adiabatic lapse rate,  $c_p$  is the specific heat at constant pressure for dry air,  $c_l$  is the specific heat at constant pressure for liquid water,  $T$  is the temperature,  $g$  is gravity, and  $q_w$  is the total liquid water mixing ratio plus saturation mixing ratio. Equa-

tion (2) is derived from the expressions for  $N_m^2$  provided in Emanuel (1994) and Kirshbaum and Durran (2004) but with the vertical gradients of  $\theta_e$  and  $q_w$  separated.

At  $t = 9$  h (Fig. 14a), there were two regions of negative  $N_m^2$  (given by the solid contours): one over the Po Valley and the other upstream of the Apennines. A budget analysis of (2) reveals these regions of  $N_m^2 < 0 \text{ s}^{-2}$  developed due to an increase in the vertical gradient of  $\partial \theta_e / \partial z$  [term A in Eq. (2)]. During the ensuing 4 h (Figs. 14b,c) convection developed in these regions of moist instability. While the convection upstream of the Apennines remained vigorous throughout the remainder of the simulation, the convection over the Po Valley waned (Figs. 14c,d). This reduction to the convective activities over the Po Valley occurred in con-

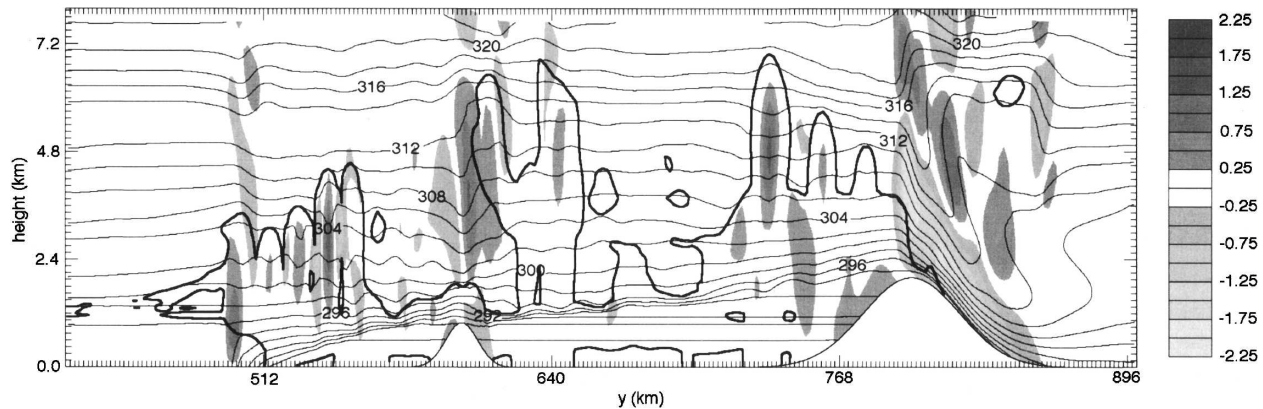


FIG. 12. Vertical cross section of potential temperature (thin contours), vertical velocity (shaded as in legend), and total liquid, ice, and snow mixing ratio =  $0.03 \text{ g kg}^{-1}$  (thick contours) at  $t = 20 \text{ h}$  for the STB10 simulation.

junction with an effective blocking of high  $\theta_e$  air past the Apennines. At  $t = 13 \text{ h}$  (Fig. 14c), downward winds induced to the lee of the Apennines advected the lower  $\theta_e$  air at midlevels downward, severing the tongue of high  $\theta_e$  air that had previously extended as far north as  $y = 750 \text{ km}$  (Figs. 14a,b). By  $t = 15 \text{ h}$  (Fig. 14d), most of the warm air to the north of the Apennines had diminished. Convection ceased above the Po Valley soon afterward.

There are two important questions regarding the above discussion. The first of these is, what role did moist processes play in the formation of the mountain-induced wave to the lee of the Apennines? To test this, a simulation identical to the STB10 simulation only with zero relative humidity in the initial sounding was performed. In this simulation, a lee wave did develop (not shown), but with an amplitude that was considerably smaller than that in the STB10 simulation. From this, we can conclude that moist processes aided in the amplification of the wave. The second question is: was the region of low  $\theta_e$  air that developed to the lee of the Apennines due to downward advection by the lee wave, or was it the result of convective stabilization? To answer this question, another simulation identical to the STB10 simulation was performed, only with the thermal effects of latent heating and cooling neglected. In this simulation, a high amplitude lee wave developed just downstream of the Apennines (not shown). This lee wave appeared to block the northward progression of high  $\theta_e$  air as in the STB10 simulation. Hence, the region over the Po Valley in this simulation was characterized by near isothermal conditions as in the STB10 simulations.

Making the assumption that the liquid water mixing ratio is small compared to the saturation mixing ratio, and, therefore, can be omitted in the calculation of

$\partial q_w / \partial z$ ,  $N_m^2$  was calculated using the observed sounding from Milan at 1800 UTC 21 October (Fig. 15). In this sounding, there is a layer of negative  $N_m^2$  between 2000 and 2500 m. Other shallower layers of negative  $N_m^2$  are present at various levels in this sounding. At other sounding times on 21 October, a similar profile of  $N_m^2$  is observed (not shown). Hence, it is not impossible that the above described mechanism for the formation of

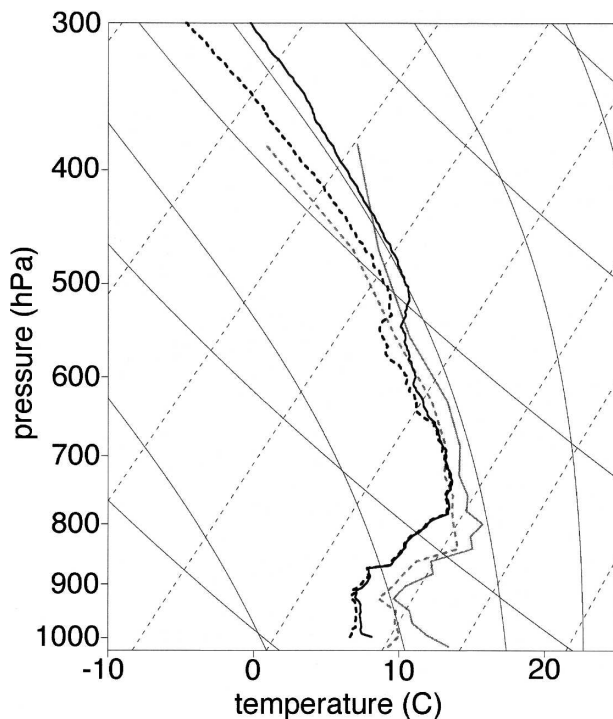


FIG. 13. Skew  $T$ -log  $p$  of observed sounding from Milan at 0600 UTC 21 October (black curves) and the model simulated sounding at  $y = 700 \text{ km}$  and  $t = 20$  for the STB10 simulation (gray curves).

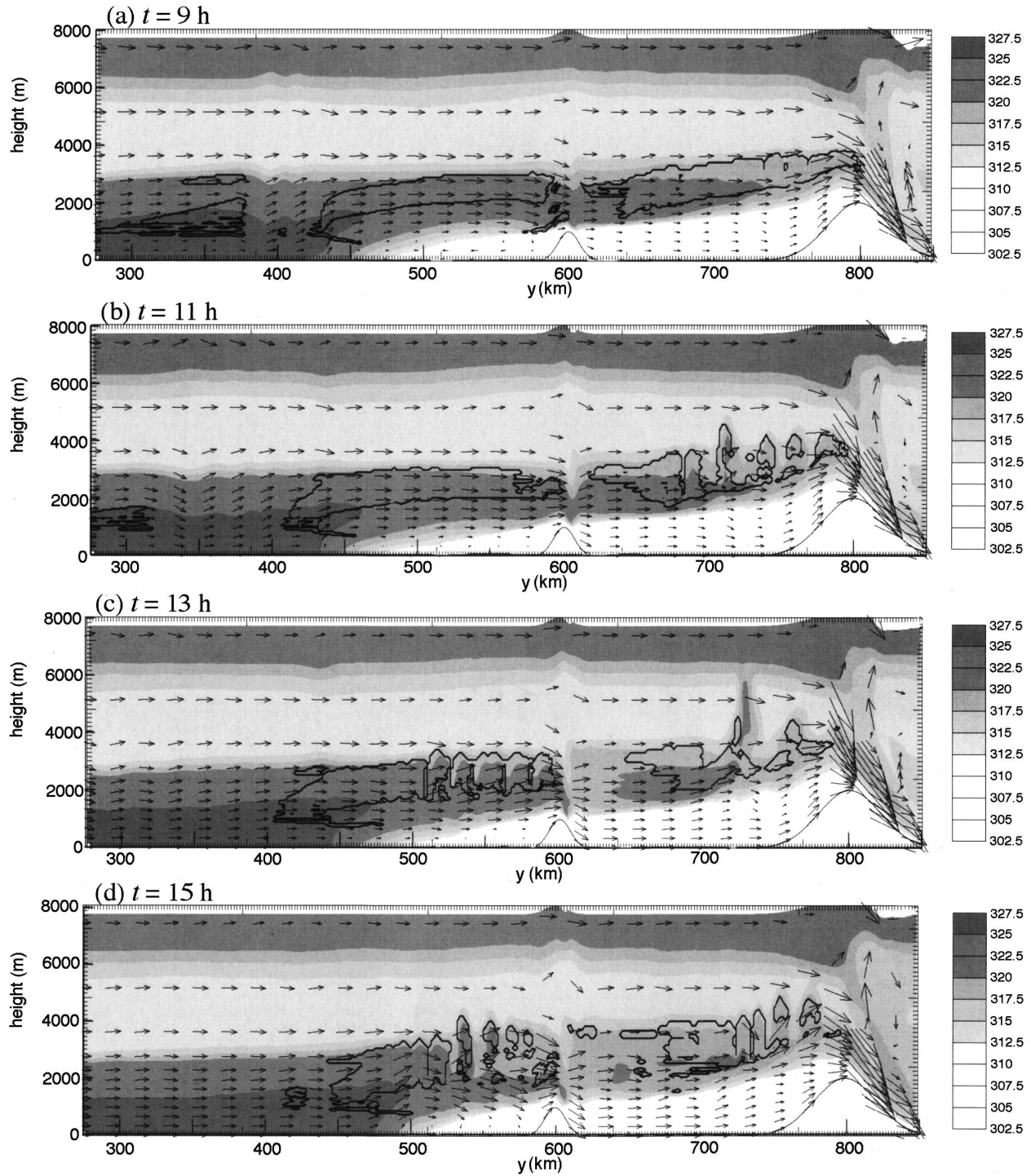


FIG. 14. Equivalent potential temperature (shaded as in legend), wind vectors, and  $N_m^2$  less than  $0 \text{ s}^{-2}$  (thick contours) for the STB10 simulation at  $t =$  (a) 9, (b) 11, (c) 13, and (d) 15 h.

convection was present in the real atmosphere. However, sufficient observations do not exist to confirm whether this mechanism was active.

Perhaps the most compelling aspect of the way in

which convection developed in the STB10 simulation is that it could not have been anticipated through examination of traditionally used upstream thermodynamic variables (Jiang 2003; Miglietta and Buzzi 2004). Re-

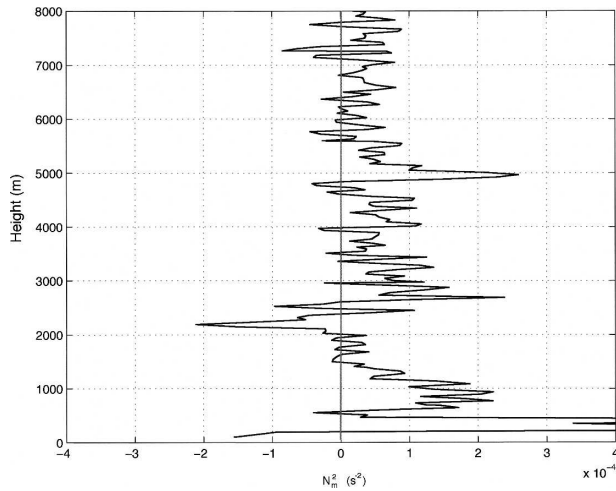


FIG. 15. Vertical profile of saturated Brunt-Väisälä frequency for the observed Milan sounding at 1800 UTC 21 October.

cently, Chen and Lin (2005a,b) proposed that the formation of convective systems over terrain is dictated by the moist Froude number ( $F_w$ ) and the convective available potential energy (CAPE) of the upstream sounding where

$$F_w = \frac{U}{N_w h}. \quad (3)$$

In Eq. (2),  $U$  is the basic state wind speed,  $h$  is the maximum mountain height, and  $N_w$  is the unsaturated, moist Brunt-Väisälä frequency (given by  $N_w^2 = (g/\theta_v)(\partial\theta_v/\partial z)$ , where  $g$  is gravity and  $\theta_v$  is the virtual potential temperature). Using the input sounding (Fig. 5), where  $U$  is  $10 \text{ m s}^{-1}$  and  $h$  is  $2 \text{ km}$ , then  $N_w$  is  $0.011 \text{ s}^{-1}$ ,  $F_w$  is  $0.46$ , and CAPE is  $9 \text{ J kg}^{-1}$ . According to Chen and Lin, such values indicate the flow over the stable layer in STB10 falls into the stratiform flow regime. This flow regime is not characterized by convection. We further note that the maximum CAPE for any parcel lifted within the lowest  $3 \text{ km}$  is  $200 \text{ J kg}^{-1}$  and that the minimum amount of lifting required to release conditional instability was  $2049 \text{ m}$  for a parcel lifted from  $z = 1360 \text{ m}$ . Such values indicate the flow was fairly stable even for large amplitude perturbations. Hence, it appears that neither traditional parcel theory nor that of Chen and Lin (2005a,b) are useful indicators of whether or not embedded cellular convection will develop within stratiform clouds. This point is related to a problem that has just started to receive attention from the scientific community (Kirshbaum and Durran 2004; Miglietta and Rotunno 2005; Furher and Schär 2005), that being the need for a control parameter based on a priori knowledge that can be used to anticipate the formation of moist unstable layers in situations of stable ascent.

Since the stable layer surrounding the Apennines in the STB5 simulation was eroded (Fig. 10), different processes controlled the evolution of convective activities. The effect of this flushing of the stable layer immediately upstream of and behind the Apennines was to reduce the half-width ( $a$ ) of the effective terrain. For the effective mountain, which is considered to be given by the shaded area in Fig. 6,  $a$  is  $100 \text{ km}$ . After the erosion of the stable layer, we can assume the effective mountain half-width is given by that of the Apennines ( $10 \text{ km}$ ). This reduction to the effective mountain half-width, corresponds to a decrease in the advective time scale, given by  $\tau_{\text{adv}} = a/U$ , from  $10\,000$  to  $1000 \text{ s}$ . These values can be compared to the buoyancy time scale  $\tau_{\text{buoy}}$ . The calculation of  $\tau_{\text{buoy}}$  herein follows the derivations presented in Kirshbaum and Durran (2004) and Fuhrer and Schär (2005) and is given by

$$\tau_{\text{buoy}} = \sqrt{\frac{k^2 + m^2}{N_w^2 k^2}}, \quad (4)$$

where  $k$ , the horizontal wavenumber, is given by  $2\pi/L$ ;  $L$  is the horizontal wavelength of the convective cells ( $12 \text{ km}$ ); and  $m$  is the vertical wavenumber. The value of  $\tau_{\text{buoy}}$  given by the above formulation is  $1200 \text{ s}$ . A comparison of this value to  $\tau_{\text{adv}}$  before the regime change noted in Fig. 9a, indicates  $\tau_{\text{buoy}}$  was less than  $\tau_{\text{adv}}$ , which implies there was time for the formation of convection. After the regime change,  $\tau_{\text{buoy}}$  was greater than  $\tau_{\text{adv}}$ . This indicates there was insufficient time for the formation of convective cells. The above formulation is of limited application since the wavelength of the convective cells is not known a priori. As mentioned above, a more desirable method would be to devise a control parameter based on a priori knowledge that can be used to anticipate the formation of moist unstable layers in situations of stable ascent.

## 5. Effective mountain argument

Lin et al. (2005) hypothesized that the stable layer in IOP-8, because it was stable with respect to both upward and downward perturbations, may have behaved as a material surface or effective mountain. Such a notion is not new. For example, Smith (1985) hypothesized that blocked layers upstream of orography could act in the same sense as terrain as far as the incident flow is concerned. This notion was later tested by Rottman and Smith (1989) who found reasonable agreement between a case where the blocked flow was replaced by a solid surface and the case where blocking occurred. Lee et al. (1989) compared the flow response for two simulations, one where a cold pool was posi-

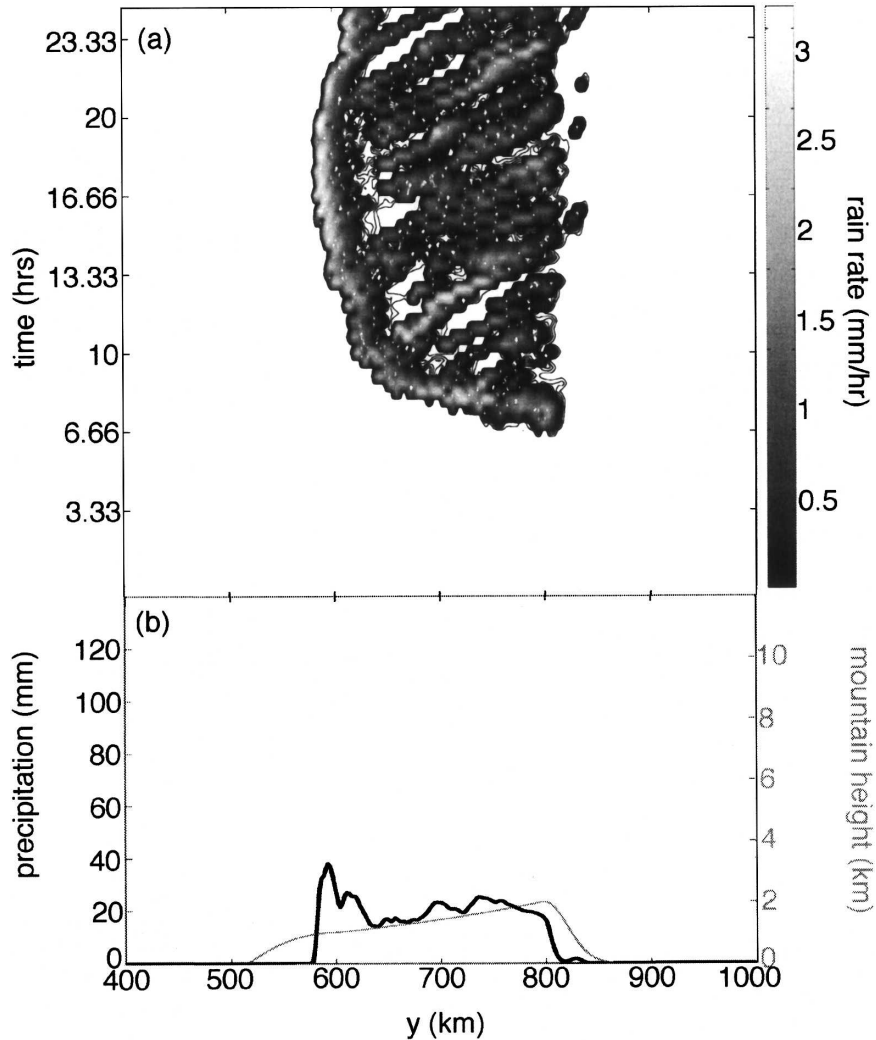


FIG. 16. (a) Hovmöller diagram of rain rate (shaded as in legend) and (b) 25-h accumulated precipitation (black curve) and orography (gray curve) for the MMTN simulation.

tioned to the lee side of a mountain and one where the cold pool was replaced by terrain. Their Figs. 5 and 6 show excellent agreement on the structure of the mountain-induced waves. Finally, Rotunno and Ferretti (2001) have argued that when low-level blocking occurs in the Po Valley, the incident southerly flow can rise over the blocked layer as though it is rising over a mountain.

If it is true that the stable layer in the STB10 simulation did act in the same manner as real terrain, then a simulation where the stable layer is approximated by actual terrain (the MMTN simulation) should yield a similar convective pattern to that in the STB10 simulation. The shaded area in Fig. 6 was used to represent the terrain for the MMTN simulation.

Figure 16a shows a Hovmöller diagram of rain rate from the MMTN simulation. According to Fig. 16a,

convection was triggered at about  $t = 6$  h between  $y = 600$  km and  $y = 800$  km. This region corresponds to the Po Valley and upslopes of the Alps in the STB10 simulation. After the convective system developed, the most vigorous convection was located at  $y = 600$  km. Individual cells propagated downstream from that location toward the modified mountain peak. The accumulated precipitation for the MMTN simulation (Fig. 16b) is consistent with the rain rate shown in Fig. 16a with a maximum of 38 mm at about  $y = 600$  km and accumulations between 15 and 25 mm across the rest of the modified mountain upslope. This precipitation pattern does not have a precipitation maximum between  $y = 550$  km and  $y = 600$  km as in the STB10 simulation.

Figure 17 shows  $\theta_e$ , wind vectors, and  $N_m^2$  for the MMTN simulation at  $t = 20$  h. Unlike that in the STB10 simulation (Fig. 14), the northward advection of high  $\theta_e$

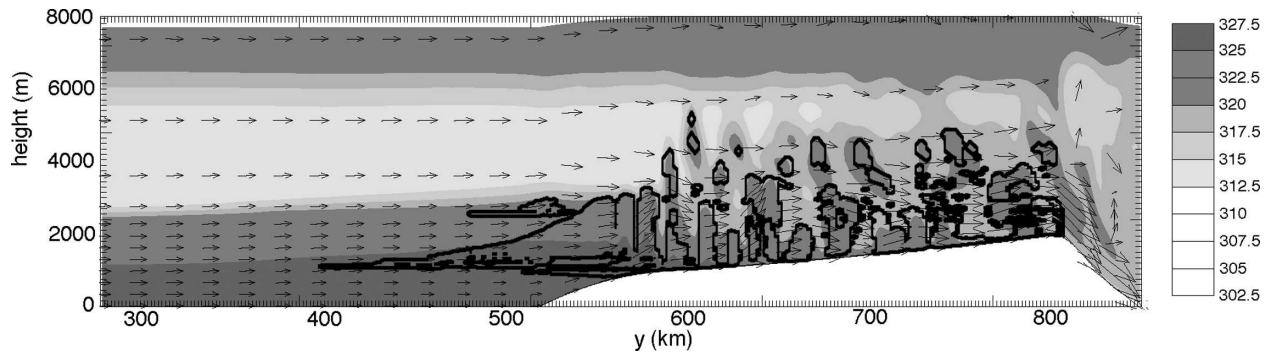


FIG. 17. Equivalent potential temperature (shaded as in legend), wind vectors, and  $N_m^2$  less than  $0 \text{ s}^{-2}$  (thick contours) for the MMTN simulation at  $t = 20 \text{ h}$ .

air was not blocked past  $y = 600 \text{ km}$  in MMTN. Throughout the duration of the MMTN simulation, air with  $\theta_e$  values in excess of  $322.5 \text{ K}$  were advected over the slope of the modified mountain as far north as  $y = 800 \text{ km}$ . The continued pumping of high  $\theta_e$  air over the upslope of the modified mountain appears to have fueled the convection over the upslope of the mountain at later times, thus allowing for longer-lived, more vigorous convection between  $y = 600 \text{ km}$  and  $y = 800 \text{ km}$  than what was observed in the same location for the STB10 simulation.

The primary difference between the MMTN and STB10 simulations is that even with a stable layer enshrouding the Apennines in STB10, there were downslope winds induced to the lee of the Apennines. No downslope winds developed on the downstream side of  $y = 600 \text{ km}$  (where the Apennines are located in the STB10 simulation) in the MMTN simulation. This result suggests that the stable layer in this case did not act in the same sense as orography. We note that the terrain used in the MMTN simulation was, perhaps, not ideal for comparison with the STB10 simulation. Inspection of Fig. 14 shows that the shape of the stable layer was not as smooth as at  $t = 0 \text{ s}$ . An additional simulation was performed in which the  $\theta_e = 312.5 \text{ K}$  isotherm was used to approximate the terrain. In this simulation, the flow patterns were not significantly different from those in the MMTN. Agreement between the MMTN and STB10 simulations may also be hampered by the lack of a return flow within the cold dome in STB10. We could not capture this return flow in our idealized simulations without violating necessary balance constraints within the two-dimensional, idealized framework.

## 6. Conclusions

Intensive observation period 8 of MAP is rather notorious for the misforecast in convective activities.

Forecast models indicated convection would occur over the Po Valley and southern slopes of the Alps. Ultimately, the precipitation in these areas was light and even. Inspection of the satellite and radar reflectivity shows that there was deep convection during IOP-8, but that it was located south of the Apennines. Radiosonde analyses show there was a cool, moist layer of air in the Po Valley and over the northern Ligurian Sea capped by a strong inversion. The inversion capping this cool layer was underestimated by the forecast models. Herein, we have investigated whether the misforecast in stable layer strength could have led to the misforecast in the placement of convection.

Observations of IOP-8 show that the flow relative to the stable layer was similar to that of flow over terrain. Lin et al. (2005) hypothesized that the stable layer behaved as an effective mountain. That hypothesis was also investigated in this paper. To meet the objectives of this research, a series of two-dimensional, idealized experiments were performed wherein the effects of the stable layer could be isolated from other processes occurring in the real atmosphere.

The effect of inversion strength on the formation of convection was tested in three sensitivity experiments with varying degrees of cooling. The first of these, the 2MTN simulation, had no initial temperature perturbation or imposed cooling in the Po Valley or upstream of the Apennines. In this simulation the maximum convection and precipitation occurred over the peak and upslope of the Alps. The STB5 simulation, which represents a case of moderate stability, was characterized by vigorous convection over the Po Valley. In the STB10 simulation, the strongest convection and greatest precipitation accumulations were south of the Apennines. Comparison of the STB10, STB5, and 2MTN simulations indicates that the stronger the inversion or stable layer, the farther south the location of maximum convection was positioned. It is not clear from this re-

search if this is an expectable result for other situations. Zängl (2005) performed a very similar study to this one using soundings with higher CAPE as well as soundings that were moist neutral. His results are different from ours. Hence, additional work considering a greater variety of upstream thermodynamic profiles is necessary to fully understand the effects of stable layers on the precipitation distribution.

In the STB10 simulation, the airstreams impinging on the effective mountain were able to ascend it in a layerlike fashion. This layerlike lifting allowed for the formation of a broad region of negative  $N_m^2$  over the upslope of the effective mountain. Cellular convection did occur in this layer. Furthermore, we have been able to demonstrate that a layer of  $N_m^2 < 0 \text{ s}^{-2}$  did exist in the real atmosphere. Hence, it is possible that the cellular convection noted in the observations (Fig. 3b) was caused by the formation of a layer of moist unstable air. This is different from the findings of Medina and Houze (2003). Their sounding analysis indicates that moist instability did not exist in the real atmosphere. Yet, their analysis is based on the averaged soundings from 1200 UTC 20 October to 2200 UTC 21 October; therefore, different results are expectable. More importantly, though, we have demonstrated that the development of convection in the STB10 simulation defies the Froude number and CAPE analyses, which indicated that the flow should have been purely stratiform. Such a finding is not new. Furher and Schär (2005) and Kirshbaum and Durran (2004) have also noted that the formation of regions of negative  $N_m^2$  in situations of stable ascent cannot be anticipated using CAPE or  $F_w$ . Since shallow, cellular convection is still capable of producing large accumulations of precipitation (Kirshbaum and Durran 2004), these results indicate a need for a control parameter based on physical data known a priori.

The presence of the Apennines in the STB10 simulation yielded a different convective pattern from that observed in Kirshbaum and Durran (2004) and Furher and Schär (2005). In the STB10 simulation, convection did not continue along the length of the stable layer throughout the duration of the simulation, reaching a quasi-steady state as in Kirshbaum and Durran (2004) and Furher and Schär (2005). Rather, convection over the Po Valley dissipated in response to downslope winds that developed to the lee of the Apennines. These winds, although not strong enough to erode the stable layer to the lee of the Apennines, were of sufficient strength to block the northward advection of high  $\theta_e$  air over the Po Valley, thus reducing the convective activities in this area. The above discussed mechanism for the formation of cellular convection in the STB10 simulation was not active in the STB5 simulation once

the stable layer surrounding the Apennines was eroded. The erosion of the stable layer in the STB5 simulation altered the effective mountain shape such that the effective mountain half-width was considerably reduced and there was inadequate time for the formation of convective cells.

The effective mountain hypothesis was tested in a simulation where the cold pool was replaced by terrain (the MMTN simulation). Although the convection in this simulation appears to have occurred as a result of layer destabilization, as in the STB10 simulation, the MMTN simulation departed from the STB10 simulation in one important regard: that being that the northward advection of high  $\theta_e$  air past the Apennines was blocked in the STB10 simulation but not the MMTN simulation. This resulted in differing convective and precipitation patterns. These results do not support the notion that the stable layer during IOP-8 acted in the same sense as real terrain.

The fact that the stable layer strength affected the development of convection is a topic worthy of additional study. Our results imply that a misforecast in stable layer strength could cause a misforecast in convection. A more thorough test of this hypothesis is necessary to confirm if such a cause-and-effect relationship exists in the real atmosphere. This could include additional quasi-idealized simulations that are three-dimensional and include more forcings that are present in the real atmosphere such as friction, a mechanism that could impact magnitude of lee waves and, hence, the location of convective activities. Given that the stable layer was so important for the redistribution of convective activities, perhaps the most logical next step is to determine more accurately what forcings caused the stable layer to persist for such an extended period of time as well as why it was not forecast accurately.

*Acknowledgments.* This research is supported by NSF Grants ATM-0096876 and ATM-0344237. We thank the following organizations for their assistance: CAPS, NCAR, NCSU-PAMS HPC, Community for Mesoscale Modeling, and the MAP Data Centre. Discussions with Richard Rotunno, Michael Kaplan, Dale Durran, and Allison Hoggarth are also greatly appreciated. We thank the three anonymous reviewers for their comments and suggestions.

#### REFERENCES

- Bougeault, P., and Coauthors, 2001: The MAP special observing period. *Bull. Amer. Meteor. Soc.*, **82**, 433–462.
- Bousquet, O., and B. F. Smull, 2003: Observations and impacts of upstream blocking during a widespread orographic precipitation event. *Quart. J. Roy. Meteor. Soc.*, **129**, 391–410.

- Chen, S.-H., and Y.-L. Lin, 2005a: Orographic effects on a conditionally unstable flow over an idealized three-dimensional mesoscale mountain. *Meteor. Atmos. Phys.*, **88**, 1–21.
- , and —, 2005b: Effects of moist Froude number and CAPE on a conditionally unstable flow over a mesoscale mountain ridge. *J. Atmos. Sci.*, **62**, 331–350.
- Crook, N. A., and M. W. Moncrieff, 1988: The effect of large-scale convergence on the generation and maintenance of deep moist convection. *J. Atmos. Sci.*, **45**, 3606–3624.
- Durran, D. R., and J. B. Klemp, 1982: On the effects of moisture on the Brunt–Väisälä frequency. *J. Atmos. Sci.*, **39**, 2152–2158.
- Emanuel, K. E., 1994: *Atmospheric Convection*. Oxford University Press, 580 pp.
- Fuhrer, O., and C. Schär, 2005: Embedded cellular convection in moist flow past topography. *J. Atmos. Sci.*, **62**, 2810–2828.
- Houze, R. A., and S. Medina, 2005: Turbulence as a mechanism for orographic precipitation. *J. Atmos. Sci.*, **62**, 3599–3623.
- Jiang, Q., 2003: Moist dynamics and orographic precipitation. *Tellus*, **55A**, 301–316.
- Kirshbaum, D. J., and D. R. Durran, 2004: Factors governing cellular convection in orographic precipitation. *J. Atmos. Sci.*, **61**, 682–698.
- Lee, T. J., R. A. Pielke, R. C. Kessler, and J. Weaver, 1989: Influence of cold pools downstream of mountain barriers on downslope winds and flushing. *Mon. Wea. Rev.*, **117**, 2041–2058.
- Lin, Y.-L., R. D. Farley, and H. D. Orville, 1983: Bulk parameterization of the snow field in a cloud model. *J. Climate Appl. Meteor.*, **22**, 40–63.
- , H. D. Reeves, S.-Y. Chen, and S. Chaio, 2005: Formation mechanisms for convection over the Ligurian Sea during MAP IOP-8. *Mon. Wea. Rev.*, **133**, 2227–2245.
- Medina, S., and R. A. Houze, 2003: Air motions and precipitation growth in Alpine storms. *Quart. J. Roy. Meteor. Soc.*, **129**, 345–372.
- Miglietta, M. M., and A. Buzzi, 2004: A numerical study of moist stratified flow regimes over isolated topography. *Quart. J. Roy. Meteor. Soc.*, **130**, 1749–1770.
- , and R. Rotunno, 2005: Simulations of moist nearly neutral flow over a ridge. *J. Atmos. Sci.*, **62**, 1410–1427.
- Raymond, D. J., and R. Rotunno, 1989: Response of a stably stratified flow to cooling. *J. Atmos. Sci.*, **46**, 2830–2837.
- Rottman, J. W., and R. B. Smith, 1989: A laboratory model of severe downslope winds. *Tellus*, **41A**, 401–415.
- Rotunno, R., and R. Ferretti, 2001: Mechanisms of intense Alpine rainfall. *J. Atmos. Sci.*, **58**, 1732–1749.
- , and —, 2003: Orographic effects on rainfall in MAP cases IOP2B and IOP8. *Quart. J. Roy. Meteor. Soc.*, **129**, 373–390.
- Smith, R. B., 1985: On severe downslope winds. *J. Atmos. Sci.*, **42**, 2597–2603.
- , and Y.-L. Lin, 1982: The addition of heat to a stratified airstream with application to the dynamics of orographic rain. *Quart. J. Roy. Meteor. Soc.*, **108**, 353–378.
- Smull, B. F., O. Bousquet, and D. Lüthi, 2001: Evaluation of real-time MC2 simulation results for a case of significant upstream blocking during MAP. *MAP Newsletter*, No. 15, Meteo Swiss, Zurich, Switzerland, 84–87.
- Steiner, M., O. Bousquet, R. A. Houze, B. F. Smull, and M. Mancini, 2003: Airflow within major Alpine river valleys under heavy rainfall. *Quart. J. Roy. Meteor. Soc.*, **129**, 411–432.
- Xu, Q., M. Xue, and K. K. Droegemeier, 1996: Numerical simulations of density currents in sheared environments within a vertically confined channel. *J. Atmos. Sci.*, **53**, 770–786.
- Xue, M., and Coauthors, 2001: The advanced regional prediction system (ARPS)—A multiscale nonhydrostatic atmospheric simulation and prediction tool. Part II: Model physics and applications. *Meteor. Atmos. Phys.*, **76**, 134–165.
- Zängl, G., 2003: The impact of upstream blocking, drainage flow, and the geostrophic pressure gradient on the persistence of cold-air pools. *Quart. J. Roy. Meteor. Soc.*, **129**, 117–137.
- , 2005: The impact of lee-side stratification on the spatial distribution of precipitation. *Quart. J. Roy. Meteor. Soc.*, **131**, 1075–1092.